Evidences of Xenon-Induced Structural Changes in the Active Site of Cyano-MetMyoglobins: A ^{1}H NMR Study

Roberto Anedda,[†] Benedetta Era,[§] Mariano Casu,*[,†] Antonella Fais,[§] Matteo Ceccarelli,[‡] Marcella Corda,[§] and Paolo Ruggerone[‡]

Department of Chemical Sciences, University of Cagliari, Monserrato-Sestu Km 0.700 I-09042, Monserrato (CA), Italy; CNR-INFM SLACS, Department of Physics, University of Cagliari, S.P. Monserrato-Sestu Km 0.700, I-09042 Monserrato (CA), Italy; and Department of Sciences Applied to Biosystems, University of Cagliari, S.P. Monserrato-Sestu Km 0.700, I-09042 Monserrato (CA), Italy

Received: July 24, 2008; Revised Manuscript Received: October 1, 2008

Using xenon atoms as a biomolecular probe raises the concern of whether they may influence in some way the molecular and electronic structure of the system under study. In this paper, the relevance of guest−host interactions in xenon complexes with paramagnetic myoglobins (Mbs) is thoroughly analyzed, and the issue about the use of xenon to detect and characterize voids within flexible biomolecules is critically discussed. A detailed ^{1}H NMR study useful for describing the hydrophobic cavities close to the active site of low-spin ferric myoglobins with respect to their interaction with the xenon atom is presented. The method is subsequently validated by the analysis of Xe-Mb with two different myoglobins, extracted from horse and pig. These myoglobins differ by 14 amino acids. One of these, Ile142 in horse Mb, is located in the proximal cavity, which is the main xenon binding site in horse Mb, and is replaced by Met142 in pig Mb. We demonstrated specific behaviors associated with the capacity of each of the two myoglobins to bind xenon and provided site-specific information on the host−guest interaction. Moreover, ^{1}H NMR measurements produce a picture of xenon-related local distortions of the protein, associated with a functionally relevant residue located right at the active site, the proximal hystidine E7(His93). According to the ^{1}H NMR data, xenon induces the tilt of the residue His93 relative to the heme plane and consequently causes an alteration of the magnetic axes. Similar conclusions are obtained both for pig cyano-myoglobin and for horse cyano-myoglobin, the structural deformation being in the former of minor entity.

Introduction

The response of a biological system to even subtle changes (e.g., physiological conditions, mutations, presence of exogenous ligands) is hard to predict, yet it is generally believed that the effects of these modifications might result in a serious alteration of the biological function involved.[1−3] This is due to the fact that biologically inspired questions are dauntingly complex for they are intrinsically many-body and many-interaction problems as well as strongly dependent on external conditions (temperature, pH, nature of the solvents, etc.). Thus, a sufficiently complete description of a biological system can be properly achieved by substantiating and complementing each single experimental technique with independent measurements or computer simulations. Obviously, the acquisition of experimental evidence plays a fundamental role in the research strategy to address biophysical and biochemical issues.

Seen in this light, a model system largely studied is not only a good benchmark for additional investigations, but the available data on it represent also a profitable source of inspiring hints to tackle open questions. Finally, the use of probes to detect and identify specific features raises the question of the guest−probe interactions, which might have implications not only on the measurement techniques but also on the functionality of the biological guest. Several of the points outlined above have motivated the research on myoglobins (Mbs) we present here.

Myoglobin is one of the most studied globular proteins and represents a paradigm of complexity. Sperm whale (SW) myoglobin was the first protein crystal structure to be solved,[4] and since then a number of different experimental and theoretical approaches have been used in order to characterize its structure and dynamics.[5−14] Single-crystal X-ray diffraction structures of myoglobins from different species and many mutants are by now well characterized to a very precise extent, and the molecular and electronic structures of these proteins have been extensively studied by using numerous complementary techniques.[15−22] Aiming to identify and characterize internal hydrophobic cavities and the effects of exogenous ligands in the crystal structures of SW MetMyoglobins (SW MMbs), Xe−MMb complexes were first solved by Schoenborn and co-workers in 1965[5] and then further investigated by Tilton et al.[6] These studies evidenced the presence of four xenon binding sites in SW MMb (Figure 1).

Among the number of studies concerning myoglobins, those focused on the role of their internal hydrophobic cavities have recently stimulated a renovated scientific interest, within the framework of the very intense and general debate on hydrophobic voids in biomolecules. Both computational studies[6−8,13,14] and laser photolysis studies as well as time-resolved crystallography[9−11] have enlightened the key role of Mb cavities in ligand dynamics. The competition with xenon in occupying these strategic sites has also been exploited for testing possible routes followed by the ligands inside the protein.[9,23] Analysis of ^{129}Xe

* Corresponding author: Ph +39-070-6754416; Fax +39-070-6754388; e-mail mcasu@unica.it.
[†] Department of Chemical Sciences.
[§] Department of Sciences Applied to Biosystems.
[‡] CNR-INFM SLACS, Department of Physics.

10.1021/jp807959u CCC: $40.75
Published on Web 11/14/2008

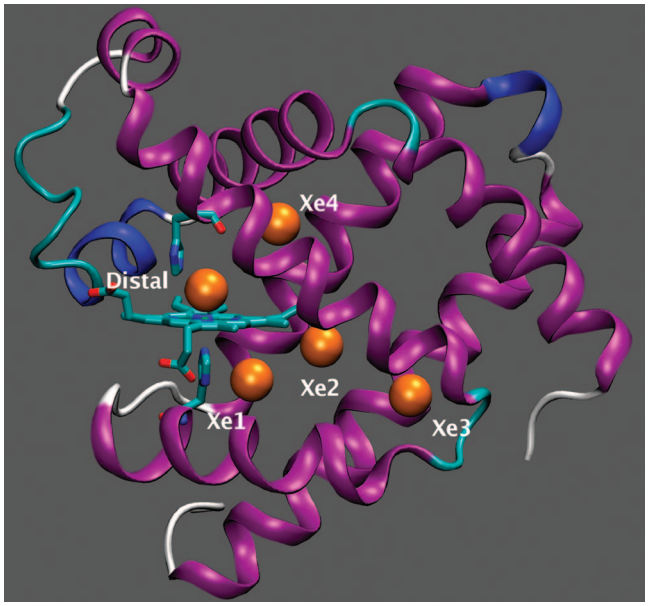

Figure 1. Schematic view of the myoglobin structure with distal and xenon cavities (the centers of mass of the cavity are represented as orange balls). The histidines 64 and 93, as well as the heme group, are also shown.

NMR chemical shifts and spin−lattice relaxation time in solutions of Xe−MMb complexes has been also used to unveil structural information on the internal cavities in proteins.[24−28] The existence of hydrophobic sites can also be inferred from the determination of the influence of xenon concentration on the protein ^{1}H, ^{13}C, and ^{15}N chemical shifts.[28−30]

Among the many concerns that are implied in using xenon atoms as a biomolecular probe, the possible influence of the probe on the molecular and electronic structure of the system under study is of principal interest for essentially two reasons: first, the suitability of xenon as a probe for the characterization of void spaces within biomolecules and/or materials implies that the influence of the probe on the host structure should be negligible or quantitatively well assessed; second, being xenon chemically inert, it is expected not to significantly modify the structure and function of the host. However, xenon-induced non-negligible structural perturbations of the host matrix have been already pointed out in several publications.[31,32] In particular, it has been observed that xenon induces the activation of some enzymes in the absence of substrates[33,34] and increases enzymatic reaction rates.[35] Recently, ^{13}C chemical shift changes due to significant xenon-induced structural modifications of the host have been also observed in flexible microporous solids.[36]

These observations, the well-known anesthetic properties of xenon[37,38] and the great debate on molecular details involved in the action of general anesthetics,[37−42] lead to the necessity of a further investigation of the effects of xenon inclusion in proteins also to possibly fine-tune these effects for exploring new features.

A related question regards the specificity of xenon binding to cavities. In fact, previous analysis showed that xenon affinity for myoglobin cavities varies depending on size, shape, and chemical composition of the cavities where it is complexed in.[9,43] However, it is still unclear which structural and physical−chemical characteristics mainly determine the affinity of xenon atoms for cavities and/or pores. Further studies are therefore strongly desirable in this sense.

To contribute to the clarification of the issues above-mentioned, we have focused our attention on myoglobins from horse and pig in the low-spin cyano ($S = {}^{1}/_{2}$) form (CNMbs). These myoglobins differ by 14 amino acids, mostly located on the protein surface. Only one difference involves the proximal cavity with the isoleucine 142 (Ile142) in horse Mb replaced by a methionine (Met142) in pig.[44]

In CNMbs most ^{1}H signals of the residues in the active site have been unambiguously assigned due to the excellent resolution and narrow ^{1}H NMR lines even for the protons close to the iron.[15−22] In these systems a significant magnetic anisotropy is present that imposes large dipolar shift to nonbonded residues in the active site and enables iron paramagnetism to probe the geometry of distal and proximal regions of the heme cavity. The study of myoglobins from pig and horse in the low-spin state points out the ability of xenon to induce non-negligible structural perturbations at the active site and permits to explain how the host−guest interaction is influenced by specific structural features of the active site in different myoglobins.

Experimental Methods

The preparation procedures as well as the experimental setups are described in detail elsewhere.[43] Here we briefly sketch some steps of the aforementioned procedure. Xenon gas at natural isotope abundance (purity of 99.99%) was purchased from SIAD (Italy) and xenon (90.9% ^{129}Xe, 99.95% purity) from Chemical Research 2000, Italy. Wilmad high-pressure NMR tubes (o.d. 10 mm and i.d. 7.1 mm, o.d. 5 mm and i.d. 4.2 mm) were used for all measurements.

Sigma furnished salt-free crystallized and lyophilized horse skeletal muscle MMb. All the MMbs (wild type) were isolated and purified according to the Wittenberg method[45] modified as described previously.[43] The purity of the Mbs was checked by sodium dodecyl sulfate−polyacrylamide gel electrophoresis (SDS-PAGE) under reducing conditions according to the classical procedure.[46]

The CNMb solutions were prepared from the MMbs by adding the cyanide sodium (Sigma) in a large excess over the heme. After the reaction, the excess cyanide sodium was removed by mild dialysis with H_2O/NaOH pH 8.0. The UV−vis spectra of aqueous CNMb samples, in the absence of xenon, show the typical features of a low-spin hemoprotein with absorption maxima at 422 and 540 nm.[47] The Mb solutions were freshly prepared at room temperature by dissolving the protein in a phosphate buffer 0.01 M, 20% D_2O. The exact protein concentration was determined spectrophotometrically at $\lambda_{max} =$ 280 nm ($\varepsilon = 31\,000\ M^{-1}\ cm^{-1}$). Samples were degassed on a vacuum line without freezing to avoid protein denaturation. Up to 10 atm of xenon gas was pressurized into the samples at room temperature. Before acquiring the spectra, the samples were equilibrated for 1 h.

Horse and pig carbon monoxymyoglobins (COMb) were prepared as described previously.[43] To test the oxidation status of the samples, we used the absorbance at 540 and 579 nm for COMb and at 502 and 630 nm for MMb. The COMb solution was prepared in a drybox and then transferred to Wilmad high-pressure NMR tubes, only in the case of total absence of MMb bands. Sample was degassed of argon on a vacuum line without freezing. Up to 10 atm of xenon gas was pressurized into the sample at room temperature. At the end of the experiment session, the analysis of the UV−vis absorption spectrum verified the oxidation status of the protein. In all the samples, the content of MMb was lower than 4%.

We recorded ^{129}Xe NMR spectra on a Varian VXR-300 spectrometer at a resonance frequency of 82.968 MHz. The chemical shift measurements were carried out at 25.0 ± 0.1

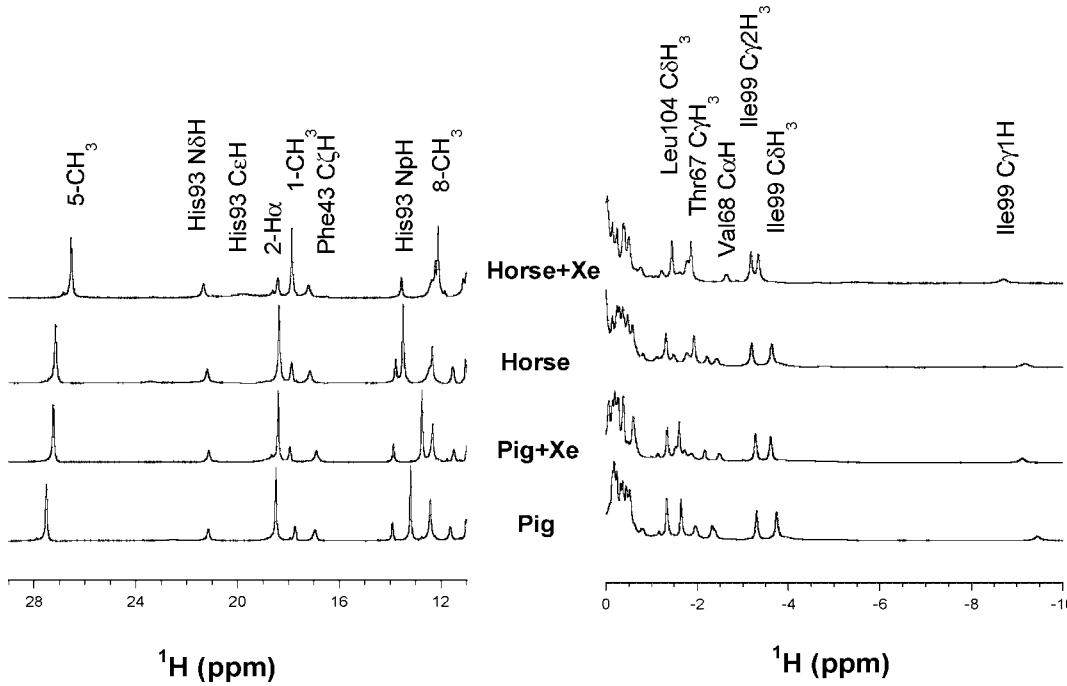

Figure 2. ^{1}H NMR spectra in the low and high field regions for ~1 mM solution of horse and pig CNMb in the absence and presence of 10 atm of xenon. Labeling of some signals is made on NOESY based on the assignments of Emerson and La Mar.[15,16]

°C, using 21 μs pulse (90°), 0.5 s repetition time, and spectral width of 20 kHz. The chemical shift of xenon (1 atm xenon overpressure) dissolved in a phosphate buffer solution (10 mM, pH 7.5) containing 20% of D_2O was taken as ^{129}Xe chemical shift reference. Each experiment run, consisting of 10 and 12 points, lasted 4 days. Before and after each experimental session, a buffer solution containing 1 atm of xenon was run, and the ^{129}Xe chemical shift was checked in order to ensure that the measured values were not caused by artifacts.

Titration data were obtained by a nonlinear fitting procedure by means of the Kaleidagraph 3.1 program; the reported errors were estimated from fitting errors. The number of scans recorded varied from spectrum to spectrum to achieve a good signal-to-noise ratio ($6 < S/N < 10$ in the spectra with 1 atm of xenon overpressure, $S/N > 10$ in all the others).

We collected ^{1}H NMR spectra on a Varian Unity-Inova spectrometer at a resonance frequency of 399.948 MHz and at $T = 28 \pm 0.1$ °C. The experiments were carried out on a 5 mm high-pressure tube using 7 μs pulse (90°), 1 s repetition time, and spectral width of 100 kHz. Chemical shifts in all spectra are referenced to DSS (2,2-dimethyl-2-silapentane-5-sulfonate) through the residual solvent signal. CNMb solutions were ~1 mM in 100 mM sodium phosphate, pH 7.5. Each experiment session, corresponding to 11 points, took 6 days.

The magnitude COSY[48] spectra were acquired in D_2O over a spectral window of 20 000 Hz using 4096 t2 complex points. We performed 128 scans for each block with a total of 1024 t1 blocks. The acquisition time was 0.102 ms, and the total acquisition time was ~20 h. The residual H_2O was suppressed by preirradiating the water signal for 0.5 s. Phase-sensitive NOESY[49] spectra were collected in H_2O. 10% D_2O was added for the lock, over a spectra window of 20 000 Hz using 4096 t2 complex points. Each of the 512 t1 increments was sampled by 128 scans. The mixing time was 50 ms with a repetition delay of 0.102 ms, resulting in a total acquisition time of 12 h. The preirradiating treatment of the water signal was carried out for 0.5 s. Phase-sensitive TOCSY spectra[50] were acquired in D_2O over a spectra window of 20 000 Hz using 4096 t2 complex points; 64 scans were collected for each block with a total of 916 t1 blocks. The spin lock time used was 50 ms with a recycle time of 0.6 s using the MLEV-17 mixing scheme. Suppression of the residual H_2O signal was obtained by preirradiating the water signal for 0.5 s.

Steady-state NOEs were carried out by selectively saturating a desired peak for 200 ms. The spectra were recorded with 10K−20K transients, 20 kHz spectral width, and 40K data points. The signal/noise ratio of the spectrum was improved by apodization which introduced 20 Hz line broadening. The percentage NOE was calculated by integrating the area of peak under consideration relative to the area of the saturated peak.

Results and Discussion

^{1}H NMR of Xe−CNMb Complexes for Identifying and Characterizing Host−Guest Interactions in Paramagnetic Myoglobins from Horse and Pig. Figure 2 collects ^{1}H NMR spectra of CNMbs from horse and pig and shows the effect of 10 atm of xenon on the chemical shifts of hyperfine-shifted protons. It is evident, even at a first sight, that the presence of 10 atm xenon overpressure causes marked changes in the proton NMR spectra. Tables 1 and 2 list the ^{1}H chemical shift of CNMb from horse and pig in the absence and presence of 10 atm of xenon, compared to the chemical shift of the corresponding protons in SW CNMb.

Note that the pioneering NMR studies of Shulman and co-workers[32] on the interaction of xenon with SW myoglobin in the low-spin cyano form in solution evidenced a significant xenon-induced chemical shift variation of just one proton signal pertaining to a methyl of the heme group. Besides this latter, most of the hyperfine shifted proton signals in the horse CNMb (see Figure 2 and Tables 1 and 2) are remarkably shifted upon addition of 10 atm of xenon overpressure in the tube. The same behavior is observed, although less pronounced, in the ^{1}H NMR signals of pig CNMb. This trend can be even emphasized when ^{1}H NMR chemical shift variation induced by xenon on proton signals assigned to residues lining the active site and/or

TABLE 1: Observed Heme ^{1}H and His93 ^{1}H Chemical Shifts (ppm) of Pig CNMb and Horse CNMb with and without 10 atm of Xenon[a]

		chemical shift (ppm)				
resonances	proton	sperm whale	horse	horse/Xe	pig	pig/Xe
heme						
	1-CH_3	18.62	18.37	17.87	18.49	18.41
	3-CH_3	4.76	4.39	3.82	4.04	3.88
	5-CH_3	27.03	27.16	26.54	27.52	27.24
	8-CH_3	12.88	13.49	12.17	13.20	12.75
	2-H_α	17.75	17.88	18.43	17.75	17.95
	2-$H_{\beta c}$	−1.73	−1.49	−1.76	−1.36	−1.52
	2-$H_{\beta t}$	−2.55	−2.42	−2.64	−2.37	−2.50
	4-H_α	5.50	5.53	5.75	5.72	5.62
	4-$H_{\beta c}$	−1.95	−1.77	−1.24	−1.97	−1.73
	4-$H_{\beta t}$	−0.77	−0.59	−0.10	−0.81	−0.61
	6-H_α	9.18	9.27	9.84	9.23	9.47
	6-$H_{\alpha'}$	7.35	7.52	8.10	7.86	8.00
	6-H_β	1.67	1.58	1.78	1.26	1.39
	6-$H_{\beta'}$	−0.48	−0.41	−0.76		
	7-H_α	1.13	1.43	1.64	1.14	1.20
	7-$H_{\alpha'}$	−0.45	−0.33	−0.01	−0.35	−0.27
	7-H_β	1.55	1.49	1.32	1.33	1.41
	7-$H_{\beta'}$	0.78	0.50	0.62	0.71	0.65
	H_α	4.40	4.41	2.60	4.32	4.21
	H_β	2.09	2.38	2.94	2.55	2.69
	H_γ	5.98	6.08	6.73	6.32	6.05
	H_δ	4.40	4.13	3.79	3.99	3.79
His93						
	$C_\alpha H$	7.51	7.41	7.49	7.49	7.48
	$C_\beta H$	11.68	11.54	11.13	11.61	11.59
	$C_\beta H'$	6.34	6.46	6.33	6.45	6.45
	$N_p H$	13.20	13.78	13.57	13.92	13.88
	$C_\delta H$	−4.70	−4.80	−4.58	−5.05	−4.98
	$N_\delta H$	20.11	21.20	21.37	21.15	21.13
	$C_\varepsilon H$	19.20	18.90	19.82	18.65	18.66

[a] The assignments made here are based on the published data on the sperm whale CNMb,[15,16] which are reported for comparison, and on COSY, TOCSY, and NOESY two-dimensional spectra.

TABLE 2: ^{1}H Chemical Shifts (ppm) of Residues in the Active Site of Pig CNMb and Horse CNMb in the Absence and Presence of 10 atm of Xenon[a]

		chemical shift (ppm)				
resonances	proton	sperm whale	horse	horse/Xe	pig	pig/Xe
Leu29	$C_{\delta 2} H$	5.53			5.63	5.56
	$C_\gamma H$	3.90	3.82	3.77	4.07	4.03
Phe33	$C_\varepsilon H$	8.32	8.36	8.33	8.31	8.27
Phe43	$C_\epsilon H$	12.58	12.42	12.38	12.41	12.40
	$C_\xi H$	17.27	17.16	17.21	16.96	16.91
Phe46	$C_\delta H$	7.69	8.23	8.19		
His64	$N_p H$	8.45			8.68	8.67
	$C_\delta H$	11.61	12.40	12.37	12.43	12.34
	$N_\epsilon H$	23.70	23.46	23.31	22.57	22.56
Val67	$C_\alpha H$		2.37	2.42		
	$C_\beta H$		0.87	0.89		
	$C_\gamma H_3'$		0.09	0.10		
	$C_\gamma H_3$		−1.93	−1.86		
Thr67	$C_\alpha H$	2.47			2.52	2.51
	$C_\beta H$	2.66			2.79	2.78
	$C_\gamma H_3$	−1.59			−1.63	−1.64
Val68	$C_\alpha H$	−2.55	−2.21	−1.78	−2.32	−2.19
	$C_\beta H$	1.42	2.03	2.08	2.00	
	$C_{\gamma 2} H_3$	−0.97	−0.61	−0.54	−0.53	−0.60
	$C_{\gamma 1} H_3$	−0.81	−0.61	−0.54	−0.53	−0.60
Ala71	$C_\alpha H$	3.48	3.49	3.56	2.85	2.90
	$C_\beta H_3$	−0.12	−0.18	−0.08	−0.20	−0.20
Leu89	$C_{\delta 2} H_3$	3.25	3.18	2.87		
Ala90	$C_\alpha H$	6.50	6.46	6.52	6.55	6.54
	$C_\beta H_3$	2.63	2.66	2.66	2.79	2.78
Ser92	NH	11.04	11.04	11.03	11.01	11.00
His97	$C_\delta H$	11.07	11.03	11.01	11.02	11.00
	$C_\gamma H$	6.83	6.82	6.83		
Ile99	$C_\alpha H_3$	−3.83	−3.63	−3.34	−3.74	−3.63
	$C_\gamma H_3$	−3.46	−3.19	−3.18	−3.30	−3.28
	$C_\gamma H'$	−1.91	−1.77	−1.22		
	$C_\gamma H$	−9.60	−9.18	−8.71	−9.44	−9.18
Leu104	$C_{\delta 2} H_3$	−1.49	−1.31	−1.45	−1.36	−1.37
	$C_{\delta 1} H_3$	0.07	0.12	0.04		
	$C_\gamma H$	0.07	0.06	0.15	0.35	0.34
Ile107	$C_\gamma H_3$	−0.25	−0.36	−0.25	−0.26	−0.27
	$C_\delta H_3$	0.37	0.34	0.25	0.38	0.37
Phe138	$C_\delta Hs$	7.05	7.08	7.11	7.12	7.12
	$C_\epsilon Hs$	6.94	7.00	7.11	7.06	7.06
	$C_\xi H$	7.02	7.08	7.11	7.16	7.15
Tyr146	$C_\delta Hs$	7.20	7.41	7.48		

[a] The assignments made here are based on the published data on the sperm whale CNMb,[15,16] which are reported for comparison, and on COSY, TOCSY, and NOESY two-dimensional spectra.

belonging to the heme methyl groups is plotted as a function of the concentration of xenon in the NMR tube (see Figure 3).

The overall change of proton NMR chemical shift observed in horse CNMb upon xenon addition ($\Delta\delta$) depends on each particular proton considered and reaches for the heme methyl 8-CH_3 of horse CNMb the significant value of 1.32 ppm, which is the maximum value observed in this study. In pig CNMb the same heme methyl group exhibits a much lower shift ($\Delta\delta$ = 0.45 ppm).

In horse CNMb, 19 out of 65 ^{1}H attributed signal shift less than 0.05 ppm (26 over 58 shift less than 0.02 ppm in pig CNMb), while 36 proton signals show shift larger than 0.1 ppm (19 in pig CNMb). Twenty-one of these signals are attributed to protons of the porphyrin ring and the other 13 to protons belonging to several residues around the heme region. In pig CNMb, 59 signals have been assigned, only 19 of which shift more than 0.1 ppm. Among these, 16 signals belong to the porphyrin ring and only three signals to residues located at the active site.

In general, as it is clearly observable in Figure 3, in pig CNMb these variations have a linear trend while in horse CNMb the $\Delta\delta$s first rapidly increase at low concentration of xenon and then asymptotically reach a saturation value. The chemical shifts of two signals attributed to protons of His64, namely $N_\varepsilon H$ and $C_\delta H$, in horse CNMb (Figure 4) initially move toward the diamagnetic envelop ($N_\varepsilon H$ $\Delta\delta$ = 0.40 ppm; $C_\delta H$ $\Delta\delta$ = 0.11 ppm) up to ~4 atm of xenon overpressure and then vary in the opposite direction ($N_\varepsilon H$ $\Delta\delta$ = 0.15 ppm; $C_\delta H$ $\Delta\delta$ = 0.03 ppm, at 10 atm of xenon). These changes are unexpected since no xenon binds in the distal cavity. In pig CNMb the chemical shift associated with the $N_\varepsilon H$ proton of His64 moves with a linear dependence toward the diamagnetic envelop up to $\Delta\delta$ = 0.09 ppm at 10 atm of xenon, while no significant chemical shift change affects the $C_\delta H$ signal.

To pinpoint possible correlations of chemical shift variations with cavity occupation by xenon atoms, we associated each assigned ^{1}H signals with the residues of hydrophobic cavities identified by Tilton et al.[6] The xenon binding site Xe4 is contiguous with the distal cavity[6] and has only two residues, Leu29 and Val68, with assigned proton NMR signals. The $C_\gamma H$ proton signals of the Leu29 and those of the $C_\beta H$ and $C_\gamma H_3$ protons of Val68 shift only slightly upon addition of xenon, while the signal of the $C_\alpha H$ proton of Val68 is perturbed by the xenon overpressure and shifts toward the diamagnetic envelop ($\Delta\delta$ = 0.43 ppm at the xenon pressure of 10 atm). For the Phe33 and Phe43 proton signals small shifts were observed, while $C_\gamma H_3$ and $C_\delta H_3$ of Ile107 exhibited shifts of the order of 0.1 ppm toward the diamagnetic envelop.

A large number of assigned proton signals of the horse CNMb belongs to residues of the proximal side of the heme pocket: Leu89, Ala90, His93, His97, Ile99, Leu104, Phe138, and Ile146. In general, the protons of residues of the proximal side exhibit

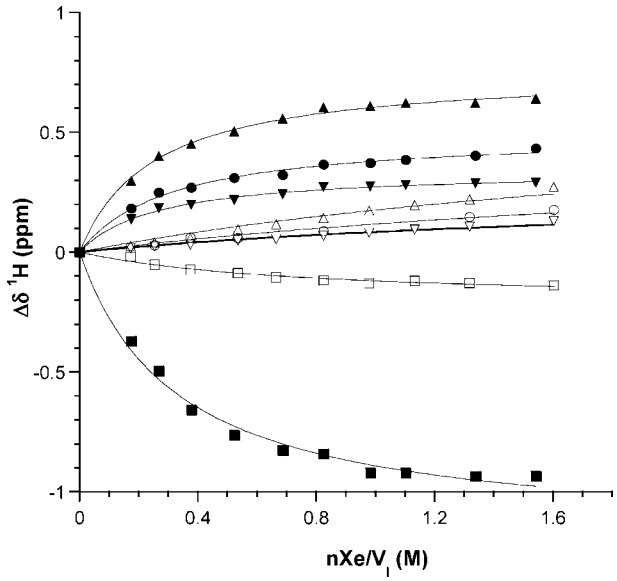

Figure 3. Total xenon-induced ^{1}H chemical shift for the horse and the pig CNMb ~1 mM at room temperature as a function of the total number of moles of xenon in the NMR tube divided by the volume of solution (nXe/V_l). The open symbols pertain to the pig CNMb while the full symbols to the horse CNMb: Heme: up triangle 5-CH_3; Ile99: down triangle $C_\delta H_3$; Val68: circle $C_\alpha H$; His93: square $C_\varepsilon H$. The data are extracted from a series of one-dimensional ^{1}H NMR spectra and/or from a series of two-dimensional NOESY spectra.

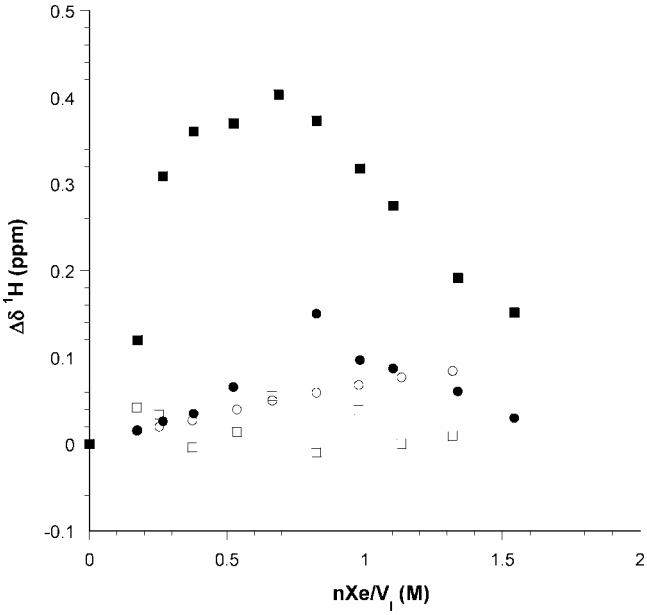

Figure 4. Total xenon-induced ^{1}H chemical shift of His64 signals is reported as a function of nXe/V_l. The open symbols pertain to the pig CNMb while the full symbols are referred to horse CNMb. Circle, $C_\delta H$; square, $N_\varepsilon H$. The data are extracted from a series of monodimensional ^{1}H NMR spectra of ~1 mM CNMb solutions at room temperature.

larger xenon-induced shift compared to those located in the distal cavity. The proximal side, also known as Xe1, is the main binding site of xenon, as pointed out by several authors.[6,26,51,52]

At this point a brief discussion of the different contributions to the experimental ^{1}H chemical shifts in myoglobins is helpful. Observed NMR shifts in paramagnetic molecules are concurrently characterized by the sum of diamagnetic, pseudocontact (dipolar), and Fermi contact contributions:[53,54]

$$\delta_{obs}=\delta_{dia}+\delta_{dip}+\delta_{con} \quad (1)$$

Here, the diamagnetic contribution δ_{dia} arises from the chemical shift (relative to DSS) of the same functional group in an isostructural diamagnetic system, the contact contribution δ_{con} results from direct delocalization of the metal unpaired spin onto the ligands of the iron, the heme and His93(F8) (the proximal histidine), and δ_{dip} is related to dipolar (pseudocontact) through-space interactions.

The pseudocontact shift δ_{dip} originates from the anisotropy in the paramagnetic susceptibility tensor and affects both ligated and nonligated residues according to the equation

$$\delta_{dip} = (12\pi N_A)^{-1}\left[\Delta\chi_{ax}\frac{3\cos^2\vartheta - 1}{R^3} + \frac{3\Delta\chi_{rh}}{2}\frac{\sin^2\vartheta\cos 2\phi}{R^3}\right]\Gamma(\alpha,\beta,\gamma) \quad (2)$$

(R, θ, ϕ) are the polar coordinates of the targeted nuclei with respect to a Fe-centered coordinate system with x and y axes lying on and z axis normal to the heme plane, $\Delta\chi_{ax} = \chi_{zz} - {}^1/_2(\chi_{xx} + \chi_{yy})$ and $\Delta\chi_{rh} = \chi_{xx} - \chi_{yy}$ are the axial and rhombic magnetic anisotropies, respectively, and N_A is Avogadro's number. $\Gamma(\alpha,\beta,\gamma)$ is the Euler rotation matrix transforming the coordinate system (x,y,z) defined above to a new one (x',y',z') in which the magnetic susceptibility tensor χ is diagonal. In particular, α is the angle between the projection of the z' axis on the heme plane and the x' axis, β describes the z-axis tilt from the heme normal, and γ represents a further rotation of the $x'-y'$ plane about z' (see Figure 5).

The three contributions to eq 1, however, have very different significance in characterizing observed proton chemical shifts in the paramagnetic myoglobins studied here. For what concerns the diamagnetic part, ^{1}H NMR experiments on the diamagnetic horse COMb in the presence of 10 atm of xenon (spectra not shown) yielded small variations (~0.05 ppm) in the δ_{dia} of the protons of His93 and porphyrin. This observation is in agreement with a relatively small effect of xenon on ^{1}H NMR chemical shift $\Delta\delta_{dia}$ (<0.1 ppm) generally observed in diamagnetic proteins,[28,55,56] including myoglobins.[32] To the best of our knowledge, the only exception is T4 lysozyme where a xenon-induced ^{1}H chemical shift change of ~0.2 ppm was observed for the protons of the residues localized mostly around the xenon binding cavity.[57] Such values are however considerably smaller than the shift observed in the present study on CNMbs. Thus, xenon-induced variations of the diamagnetic contribution to the observed proton chemical shift change are not sufficient to explain experimental results. This suggests that the observed changes should be considered merely influenced by the hyperfine interaction between the proton and the unpaired electron of the heme iron and attributed mostly to dipolar and contact contributions.

To achieve a reliable picture of the origin of xenon-induced perturbation, we have to discuss which structural features could effectively influence the observed ^{1}H chemical shifts.

The pseudocontact shift δ_{dip} affects both ligated and nonligated residues according to eq 2 and is strongly characterized by the anisotropic magnetic susceptibility tensor χ. This latter dependence is very important: the analysis of various CNMb point mutants[58−60] as well as of model compounds[61] has demonstrated that it is strictly related to structural features of the heme cavity. In this regard, some NMR studies of myoglobin

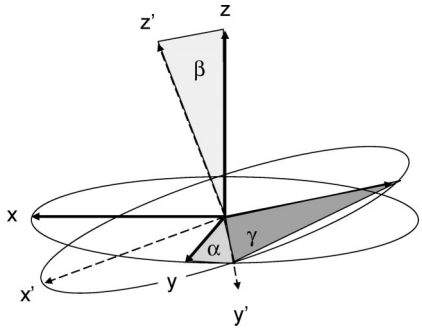

Figure 5. Pictorial representation of the Euler angles α, β, and γ, transforming the crystallographic Cartesian reference system (x,y,z) to one in which the magnetic susceptibility tensor χ is diagonal (x',y',z').

mutants have been carried out to determine the orientation of the magnetic axes.[21,62,63] It was suggested that point mutations in the distal side affect the orientation of the Fe−ligand axis (e.g., Fe−CO, Fe−CN) and, consequently, the principal axis of the magnetic susceptibility tensor (described by the angle β). Instead, mutations in the proximal side influence only the orientation of the rhombic axes of the tensor (described by the angle $\kappa = \alpha + \gamma$), either causing a rotation of the heme or of the proximal histidine.[63] In particular, a proposed critical factor of the perturbation in heme proteins is the orientation of the His93 imidazole ring with respect to the heme iron. Note that while a correlation does exist between axial His plane and rhombic axes,[16] it remains still unclear whether this correlation is the only determinant of rhombic axes orientation.

As already specified in eq 2, δ_{dip} is influenced by the orientation of the susceptibility tensor χ, which is in turn related to α, β, and γ. It is thus reasonable to associate the observed ^{1}H chemical shift patterns with a structural modification that is caused by xenon and involves a residue lining the xenon cavity, possibly influencing the orientation of the magnetic axes. It has been previously assessed,[21] in fact, that changes in the pattern of His93 ring hyperfine shifts do point toward possible alterations of the magnetic axes. Specifically, either a larger β or an increasingly positive α was found to be responsible for an upfield bias for the signal of the His93 $C_\delta H$ proton and simultaneously for a downfield bias for signals of His93 $C_\varepsilon H$ and of the four Ile99 resonances.

Aiming at finding trends of proton chemical shift variations that could be associated with a particular modification of the orientation of magnetic axes, we calculated the dipolar contribution to the chemical shift upon changing α (with β fixed) or β (α fixed). The calculation was based on eq 2 and on atomic coordinates extracted from crystal structures of the horse Mb (PDB file 1YMB), assuming $\Delta\chi_{ax}$ and $\Delta\chi_{rh}$ equal to 2.54×10^{-9} m^3/mol and -0.62×10^{-9} m^3/mol, respectively (see Supporting Information).

The calculation reveals that some of the signals show only little dipolar shift by changing either α or β, at least for the range considered; His97 $C_\delta H$, Ile99 $C_\gamma H$, and His93 $C_\epsilon H$, conversely, exhibit a large increase when both α and β assume more positive values. Hence, changes in the shifts observed for these signals cannot be used to differentiate between changes in α vs β. On the other hand, the calculated dipolar shifts of Phe43 $C_\xi H$, Val68 $C_\beta H$, His93 $C_\beta H$, Leu89 $C_\gamma H$, and His97 $C_\gamma H$ predict opposite direction for δ_{dip} changes upon increasing α and β and hence can potentially serve for discriminating between changes in α vs β.

In horse CNMb the chemical shift variations of the His93 protons $C_\beta H$ ($\Delta\delta = 0.41$ ppm upfield), $C_\varepsilon H$ ($\Delta\delta = -0.92$ ppm downfield) and the downfield shift of Ile99 ($C_\delta H_3$ $\Delta\delta = -0.29$ ppm, $C_\gamma H_3$ $\Delta\delta = -0.01$ ppm, $C_\gamma H'$ $\Delta\delta = -0.55$ ppm, $C_\gamma H$ $\Delta\delta = -0.47$ ppm) after xenon addition, consequently, could be interpreted in terms of a dependence of the shifts on the orientation of the His93 imidazole ring relative to the heme plane under xenon supply (see Figure S1 of the Supporting Information). The obtained values indicate that the trends experimentally observed for the dipolar shift of the majority of assigned protons can be attributed to a xenon-induced change toward more positive values of α rather than to a modification of β.

Inspection of the Table 2 and Figure S1 (Supporting Information) shows that the His97 $C_\delta H$, Val68 $C_\alpha H$, Val68 $C_\beta H$, and Val68 $C_\gamma H$ exhibit dipolar shift changes that support the conclusion that xenon addition causes small change in α rather than in β and that the change in α is toward a more positive value.

The variation in the α values suggests that xenon-induced non-negligible structural perturbation in the proximal side can influence the orientation of the rhombic axes of the tensor, causing a rotation of either the heme or the proximal histidine.[63]

From the above-mentioned calculations, however, it is impossible to distinguish to which extent α and γ vary, thus indicating that most likely they are simultaneously changed by the presence of xenon atoms rapidly exchanging within the cavities of Mb. It is worth noting that although many studies have been performed to characterize the orientation of magnetic axes in paramagnetic myoglobins, the methods so far proposed have reached only accuracy of about ±10° in defining α, β, and γ values; smaller changes, which however may have significant relevance in characterizing myoglobins functionality, are currently undetectable.

Thus, a reliable quantitative assessment of this dependence can potentially provide valuable structural information on local distortions in CNMbs. Moreover, any discussion of Fe−^{1}H dipolar interactions in paramagnetic proteins should additionally take into account that the observed proton signals could experience both contact and dipolar shifts simultaneously. Evaluating both contributions, and quantitatively separating them, appears a challenging but important issue in order to achieve a correct interpretation of NMR results.

Previous studies concerning low-spin ferrihemoproteins[63] have shown that the heme H_{meso} protons exhibit both contact and dipolar shifts; they also pointed out that the measured asymmetry in the H_{meso} hyperfine patterns, calculated from the equation

$$\Delta\delta_{meso} = 1/2[\delta_\alpha - \delta_\beta + \delta_\gamma - \delta_\delta] \qquad (3)$$

is quantitatively mostly influenced by the rhombic dipolar shifts, being the contact contributions to their observed chemical shift very similar to each other. Thus, calculation of $\Delta\delta_{meso}$ would lead to better understand possible rhombic (in-plane) magnetic axes displacements related to local structural rearrangements attributable to the presence of xenon. From the available data (Table 1), $\Delta\delta_{meso}$ values of 1.99 and 2.05 ppm were extracted for horse CNMb and pig CNMb, respectively, in the absence of xenon (see Table 1), in good agreement with $\Delta\delta_{meso} = 1.8$ ppm found in wild type SW CNMbs.[63] The $\Delta\delta_{meso}$ decreases to 1.3 ppm in horse CNMb and to 1.89 ppm in pig CNMb after adding 10 atm of xenon gas, thus suggesting that the rhombic axes have rotated clockwise relative to the heme and that the angle κ is to some extent increased by the presence of xenon in the proximal cavity. These observations suggest that proximal His93 has rotated counterclockwise with respect to the stationary heme, a hypothesis that can be further substantiated by NOE

measurements, as discussed in the next subsection. Additional quantitative information can be easily obtained: as previously suggested,[63] a plot of calculated $\Delta\delta_{meso}$ vs κ indicates a gradient of 2.5 ppm per 10° of rotation; this correlation enables a rough estimate of the relative rotation of the proximal histidine with respect to the heme group to be obtained. The calculation suggests a counterclockwise rotation (viewed from the proximal side) of His93 of about 2.8° in the horse CNMb and of only 0.64° in pig CNMb.

NOE Measurements Used as a Tool To Further Assess His93 Rotation Relative to Heme in Horse CNMb. The counterclockwise rotation of His93 can be easily monitored in low-spin cyano myoglobins by following the inter-residue dipolar contacts between the rotating residue (His93) and backbone protons on the E and F helices. Moreover, steady-state NOEs upon saturation of either the heme protons or the His93 protons discriminate between a rotation of the heme and a rotation of the His93, both leading to a relative displacement of one of them with respect to the other. These experiments have been carried out only on the horse CNMb because it was observed that the xenon-induced rotation of His93 in pig CNMb is nearly negligible. Figure 6a shows that the steady-state NOEs, resulting from saturating 8-CH_3 signal in horse CNMb samples pressurized with 10 atm of xenon, are essentially the same as for degassed solutions, indicating an unchanged position of the heme with respect to the protein matrix in the heme cavity.

The absence of significant changes has been confirmed by decomposing the signals into individual gaussians by means of the software package Origin 7 from Microcal (not shown). Figure 6b compares steady-state NOEs without and with 10 atm of xenon of a horse CNMb sample, obtained upon saturating His93(F8) $N_\delta H$ proton signal. The spectrum of myoglobin pressurized with xenon shows some new resonances and various modifications in signal intensities with respect to the degassed myoglobin sample. In particular, new signals appear at 11.03 and 12.10 ppm, assigned to Ser92 NH and 8-CH_3, respectively. Decreases in the intensities of the signals of Leu89 $C_\alpha H$ (∼−23%) and His93 $C_\beta H$ (∼−13%) are observed in the spectrum of the Xe−Mb complex with respect to that of the degassed solution. Moreover, the signal assigned to His93 N_pH has an increased NOE (∼+28%) after xenon addition. Considering the R^{-6} dependence of the NOE, simple calculations lead to the conclusion that His93 $N_\delta H$ is displaced by ∼4% further from Leu89 $C_\alpha H$ by the xenon atoms residing in the proximal cavity (Xe1). Since the His93 $N_\delta H$−Leu89 $C_\alpha H$ distance in the X-ray structure of horse Mb (PDB file 1YMB) is 4.25 Å, a 23% decrease in signal intensity in NOE spectra is indicative of an increase of this distance to ∼4.43 Å. In the same way it can be calculated a decrease of the distance His93(F8) $N_\delta H$−His93 N_pH of ∼4% (analogous calculations based on the crystal structures suggest a distance change from 2.99 Å before xenon pressurization to 2.87 Å after xenon addition). These observations are in very reasonable agreement with the new signals visible in the NOE spectrum of pressurized samples.

Whether this displacement is a translation of the whole F8 residue or a counterclockwise rotation (viewed from the proximal side) of the imidazole ring about the His93 $N_\varepsilon H$−Fe bond is uncertain, but the latter hypothesis is the most reasonable, given the strong Fe−His coordination bond. Further confirmation of the tilt/rotation of His93 ring toward the heme δ-meso-H comes from the observation of NOE enhancement of the proton signal belonging to 8-CH_3 after pressurization with xenon, which is not present in the absence of xenon (see Figure 6b).

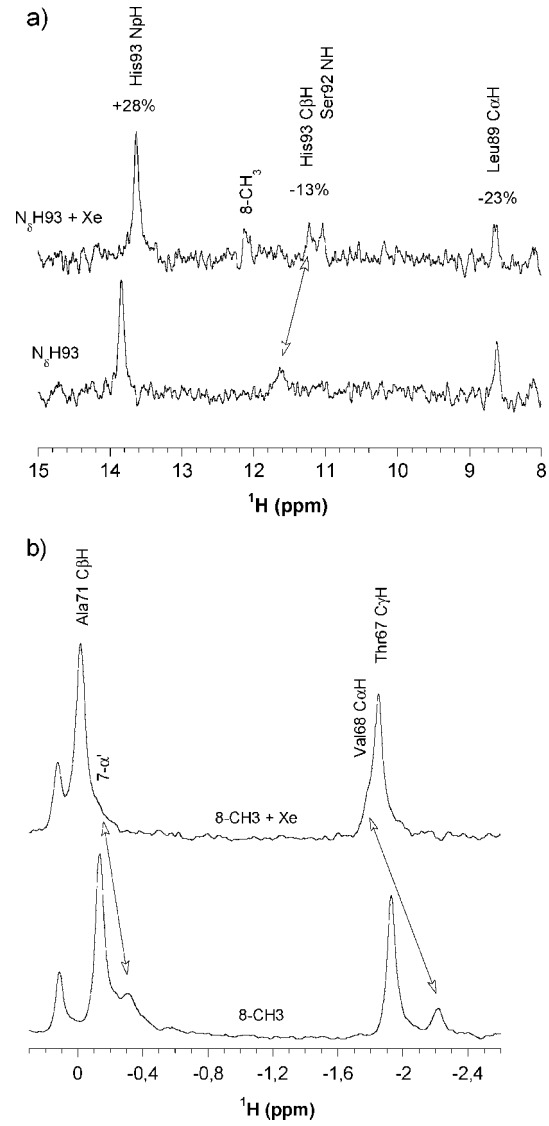

Figure 6. (a) ^{1}H NMR steady-state NOEs observed by selectively saturating the heme signal 8-CH_3 in samples of horse CNMb pressurized with 10 atm of xenon gas pressure and evacuated. (b) Steady-state NOEs observed saturating the His93(F8) $N_\delta H$ signal in solutions with and without 10 atm of xenon pressure. Some assignments are reported together with their signal intensity increase/decrease.

Thermodynamics of Xenon Binding to Cyano-Metmyoglobins from Xenon-Induced ^{1}H NMR Chemical Shift Variations. Observation of the proton chemical shift variation scheme as a function of the concentration of xenon in solutions of CNMbs from pig and horse leads to interesting considerations. For each assigned peak of the horse and pig CNMb spectra, the ^{1}H chemical shift variation, $\Delta\delta$, as a function of xenon concentration is fitted by the two-site model:[27]

$$\Delta\delta_{obs} = \frac{K[\mathrm{Xe}]}{1 + [\mathrm{Xe}]}\Delta\delta_{max} \qquad (4)$$

Here K is an equilibrium binding constant, [Xe] the xenon concentration in the buffer, and $\Delta\delta_{max}$ the chemical shift difference between the complexed and free protein (degassed solution). Interestingly, eq 4 resembles the Langmuir adsorption equation commonly used in gas adsorption on the surface of solid materials. Only the fitting results having correlation

TABLE 3: Values of the Binding Constant *K* for the Residues of Horse CNMb Extracted from the Fitting of the Correspondent ^{1}H Signals

resonances	protons	K (M^{-1})	r	resonances	protons	K (M^{-1})	r
heme	1-CH_3	126 ± 9	0.9983	heme	$C_\varepsilon H$	94 ± 8	0.9986
	3-CH_3	96 ± 9	0.9976		H_α	119 ± 10	0.9986
	5-CH_3	127 ± 10	0.9987		H_β	103 ± 10	0.9991
	8-CH_3	90 ± 3	0.9998		H_δ	80 ± 10	0.9967
	2-H_α	80 ± 7	0.9996		H_γ	90 ± 13	0.9916
	2-$H_{\beta c}$	106 ± 10	0.9995	His93	$C_\alpha H$	80 ± 6	0.9988
	2-$H_{\beta t}$	89 ± 8	0.9989		$C_\beta H$	110 ± 7	0.9991
	4-$H_{\beta c}$	85 ± 7	0.9986		$C_\beta H'$	112 ± 10	0.9991
	4-$H_{\beta t}$	94 ± 9	0.9993		$N_p H$	85 ± 4	0.9992
	6-H_α	89 ± 3	0.9997		$N_\delta H$	147 ± 11	0.9995
	6-$H_{\alpha'}$	93 ± 7	0.9992	Ile99	$C_\delta H_3$	116 ± 9	0.9978
	6-H_β	137 ± 13	0.9986		$C_\gamma H'$	133 ± 12	0.9938
	6-$H_{\beta'}$	158 ± 11	0.9995		$C_\gamma H$	80 ± 7	0.9910
	7-H_α	154 ± 15	0.9976	Ile104	$C_\gamma H$	159 ± 10	0.9981
	7-$H_{\alpha'}$	87 ± 7	0.9973		$C_{\delta 2} H_3$	145 ± 9	0.9991
	7-H_β	81 ± 8	0.9934	Ile107	$C_\delta H_3$	94 ± 9	0.9938
	7-$H_{\beta'}$	88 ± 8	0.9961	Val68	$C_\alpha H$	98 ± 9	0.9982

function F larger than 0.99 and standard error of the calculated K smaller than 10% were considered.

In the horse CNMb, 34 out of 65 ^{1}H chemical shift variations associated with proton signals are well described by the two-site thermodynamic model. Twenty-one proton signals belong to the porphyrin ring and the other 13 to several residues around the heme region. The remaining 36 ^{1}H signals shift only negligibly or show a correlation function F lower than 0.90. Table 3 contains some of the K values extracted from the fitting analysis.

The 8-CH_3 ($\Delta\delta$ = 1.32 ppm) and H_α ($\Delta\delta$ = 1.81 ppm) protons of the porphyrin ring exhibit the maximum chemical shift variations. K, as derived from the individual fitting of the 34 signals, ranges between 80 and 150 M^{-1}, while fitting all chemical shift variations on the whole (software package Origin 7 from Microcal) leads to $K = 109 \pm 7\ M^{-1}$. $\Delta\delta_{max}$ lies between 2.1 and −0.69 ppm, revealing large proton chemical shift variations when xenon is bound to the protein.

Negligible shifts or linear trends characterize the 58 assigned proton signals in the pig CNMb when xenon is added up to 10 atm overpressure in the tube. Twenty-four signals have a shift larger than 0.05 ppm, 19 belonging to the porphyrin ring and the others to the $C_\delta H_3$ and $C_\gamma H$ group of Ile99, to $C_\alpha H$ and $C_{\gamma 2} H_3$ of Val68 and to $C_\delta H$ of Val64. The maximum $\Delta\delta$ is associated with the 8-CH_3 ($\Delta\delta$ = 0.45 ppm) and H_α ($\Delta\delta$ = 0.37 ppm) protons of the porphyrin ring (see Table 3). Using eq 4 to fit these chemical shift variations, we estimate a binding constant K lower than 5 M^{-1} for pig CNMb samples, to be compared with $K = 109\ M^{-1}$ obtained for the horse CNMb.

General Remarks on Xenon Binding to Myoglobin Cavities. For horse and pig MMbs (high-spin Fe^{3+}) ^{129}Xe NMR was used by Corda et al.[43] to evaluate the sensitivity of xenon to local environments by monitoring the ^{129}Xe shift and the spin−lattice relaxation rate. Their study evidently supported the role of the Xe1 cavity as the main xenon binding site in the horse MMb, while in the pig their findings indicated the presence of more than one xenon binding site besides Xe1. The different behavior of ^{129}Xe NMR was attributed to structural differences in the Xe1 cavity: Ile142, present in the horse Mb and located on the opposite side of the heme group, in the pig Mb is substituted by Met142 with a longer side chain. The substitution influences the xenon binding and consequently the xenon population because it reduces (a) the size of the Xe1 cavity bringing in the pig MMb the center of gravity (CG) closer to the iron (distance Fe−CG = 4.9 Å), than in the horse (Fe−CG = 5.3 Å),[43] and (b) the hydrophobicity of the cavity because the methionine is not as highly hydrophobic as the isoleucine and xenon is known to prefer hydrophobic regions.[64]

The present study has pointed out and quantitatively discussed the influence of guest molecules on the structure of the host, in our case horse and pig Mbs. The proton chemical shift variations observed in the horse CNMb have been directly correlated to changes in the orientation of the principal magnetic axes of the Xe−CNMb complexes. Besides complementing ^{129}Xe NMR results with site-specific information, ^{1}H NMR measurements produce a picture of xenon-related local distortions of the protein. These structural modifications of the protein induced by the guest atom are spotlighted and associated with a residue located right at the active site. According to the ^{1}H NMR data, xenon induces the tilt of the residue His93 relative to the heme plane and consequently causes an alteration of the magnetic axes.

Similar conclusions are obtained also from the ^{1}H NMR data on pig CNMb. Here, the analysis of the ^{1}H NMR measurement confirms a similar picture as that in horse CNMb, but of minor entity. The result, in agreement with the previous study on horse and pig MMb, points to xenon atoms occupying the Xe1 site in pig CNMb, which however results less populated than it is in the horse CNMb.

The induced tilt of the residue His93 relative to the heme plane and the consequent alteration of the magnetic axes induced by xenon in the Xe1 cavity have, in our opinion, very general consequences, since structural modifications of the cavities and structural perturbations of the ligand tilt could affect the kinetics of ligand binding but also determine relative affinities and consequently the physiological function of the myoglobins.

It is in fact recognized that proximal histidine has an important role in modulating the reactivity of heme proteins: several techniques have provided evidence that a displacement of proximal histidine upon ligand dissociation, also referred to as *doming* vibrational mode, strongly affects the reactivity of this type of biological molecules.[65−67] Proximal histidine acts as a trigger for structural changes leading to cooperative transition in hemoglobin.[65] It has also been shown that CO binding kinetics are modified in proximal mutants of myoglobins with respect to wild type.[28,63] Additionally, the hydrogen bond linking the hydroxyl group of Ser92 to the $N_\varepsilon H$ of His93 has an important role in the protein activity.[69,70] In this regard solution studies have yielded different results with respect to crystal structures

likely due to the existence of some substates[71] in the structure of the proximal region of myoglobin.

It must be recognized that while the tilt/rotation of His93 ring can explain the shifts of the residue observed after pressurization with xenon in the distal and proximal cavity in horse CNMb, this cannot give reliable justifications of the shift of the $N_\varepsilon H$ and $C_\delta H$ of His64 (see Figures 4 and 5 as well as Figure S1 in the Supporting Information). The His64 residue belongs to the distal cavity and is one of the most important residues controlling the ligand binding reaction of myoglobins and, as proposed by computational studies, seems to be involved in the escape route of the ligands, the so-called "E-helix gate".[72] The observed shifts can be attributed to some movement of the imidazole ring, likely associated with its rotation, and they can be better understood by taking into account the following considerations:

(1) Such unexpected behavior might hypothetically arise from the presence of significant population of xenon in the Xe4 cavity at xenon overpressure larger than 4 atm. The Xe4 cavity, which is on the distal side close to the oxygen-binding cavity, is relatively close to the iron (its center of gravity is 8.4 Å from Fe) and is not in contact with the heme group. From calculations using the software VOIDOO the Xe4 cavity turns out to be larger in pig (25.8 $Å^3$) than in horse (19.7 $Å^3$) but smaller than the Xe1 cavity in both proteins.[43] A previous crystallographic work has demonstrated that Xe4 site is populated ~10 times less than the Xe1 site in sperm whale Mb.[6] The signals of the residues lining the Xe4 cavity show small shifts in both proteins in presence of xenon, while the signal attributed to the $C_\alpha H$ proton of Val68 in horse CNMb ($\Delta\delta = 0.43$ ppm, 10 atm of xenon) undergoes a non-negligible variation. However, the presence of xenon in the Xe4 cavity in pig would be expected to cause more significant shifts of the signals assigned to $N_\varepsilon H$ and $C_\delta H$ of His64. However, such an effect is not observed.

(2) It has been ascertained that there are possibly several conformations relative to the His64 residue in solution. Yang and Philips, Jr.,[73] by a X-ray crystallographic study at various pH values, have shown that there are two major conformations of Mb, which are referred to as *open* and *closed*. The His64 $\chi 1$ angle (the dihedral angle around the C_α and C_β) of the open conformation at neutral pH is larger by ~100° than that of the *closed* one at acidic pH. Thus, another possible effect of xenon on myoglobin structure is that, besides modifying the tilt/rotation of His93 ring, it may affect the just mentioned conformational equilibrium by influencing the binding of the cyano group and then restricting some movements of the His64 imidazole.

(3) Earlier attempts to determine the orientation of the magnetic susceptibility tensor in low-spin cyano myoglobins by exploiting calculated ^{1}H NMR dipolar shifts and observed hyperfine shifted proton resonances evidenced an unusual behavior associated with His64 (E7) and Val 68 (E11).[16] In particular, in the calculation procedure involving all the assigned protons, it was noted that a significant improvements of the results could be obtained upon omitting experimental shifts observed for protons of E11 and E7. The problem evidently derives from an intrinsic incongruence between the calculated and the experimental hyperfine shifts relative to protons associated with these residues, taking into account that the existence of an electronic interaction between the iron and His64 $N_\varepsilon H$ has been already demonstrated.[74] Moreover, the His64 $N_\varepsilon H$ labile proton, which is hydrogen bonded to cyanide ion in CNMb, most likely experiences a contact shift contribution through the spin density of the cyanide nitrogen,[75] this fact determining its complex and hardly predictable NMR shifts.

All these considerations, although unable to fully explain the experimental trends observed for the protons of the residues His64 (E7) and Val68 (E11), shine a light on the complexity of the multiple factors that simultaneously characterize their NMR parameters. What clearly appears, in conclusion, is that anyway these two residues cannot be reliably considered local indicators of the presence of xenon in the Xe4 cavity. Because of its undersized volume with respect to xenon and the consequent large shift expected but not observed for almost all the residues (other than E7 and E11) lining the cavity, it is safe in our opinion to conclude that the Xe4 is not significantly populated in solution in the interval of xenon pressure studied.

Generally, both steric factors and particularly hydrophobic interactions are supposed to regulate ligand diffusion and binding inside Mbs.[76] The process of identifying possible ligand pathways inside the protein would be greatly enhanced by knowing to what extent each concurrent ligand−protein interaction influences the affinity of the ligand for a particular site. In this regard, recent computational studies by Cohen et al.,[76] aimed at describing migration pathways for small ligands inside Mbs across different animal species, have highlighted strong similarities between the diffusion of O_2 inside pig and SW Mbs. The present work confirms the just mentioned computational results and additionally gives experimental evidence that distribution of the atomic probe xenon is significantly influenced by the residues lining the possible xenon binding sites and points to a differentiation of hydrophobic cavities within pig and horse myoglobins concerning their capacity to bind xenon.

Cohen and co-workers, however, while giving an interesting input for further studies, performed only a qualitative investigation and pointed out that more studies were desirable in order to assess weather their result was coincidental and to deeper understand the role of Mb structure and dynamics in providing ideal energy profiles for ligand diffusion. In this light, our findings represent a novel interesting starting point for guiding further computational approaches to the problem.

Conclusion

In the present work we carried out a detailed discussion of a ^{1}H NMR study useful for describing the hydrophobic cavities close to the active site of paramagnetic myoglobins with respect to their interaction with an ideal atomic probe, the xenon atom. It is commonly believed that these cavities, far from representing structural imperfections of the macromolecular framework,[77,78] play a fundamental role in the protein functionality by finely modulating ligand binding and/or diffusion throughout the internal regions of the biomolecule.

By analyzing two different myoglobins, extracted from horse and pig, we demonstrated specific behaviors with respect to their capacity to bind xenon and provided site-specific information on the host−guest interaction.

The agreement between previous ^{129}Xe NMR measurements on high-spin Met-Mbs from horse and pig[43] and ^{1}H NMR findings discussed here indicates the presence of xenon in the Xe1 cavity in both myoglobins, thus validating and complementing earlier works with local information on the active site of myoglobins.

It is demonstrated that in horse myoglobins the presence of xenon in the Xe1 cavity induces the tilt of the residue His93 relative to the heme plane and consequently an alteration of the magnetic axes. This structural modification evidence that

xenon, being chemically inert, is able to induce non-negligible structural perturbations at the active site of these proteins, which may cause interference with their function. Structural perturbations of the His93 tilt could not only affect the kinetics of ligand binding but also determine relative affinities and consequently the physiological function of the myoglobins. In this light, it is worth noting that guest-induced deformations of the host matrix, even apparently negligible ones, should be quantitatively assessed and critically evaluated.

Acknowledgment. This study was supported by Fondo per gli investimenti della ricerca di base (FIRB-RBAU014H98) and makes use of results produced by the Cybersar Project managed by the Consorzio COSMOLAB, a project cofunded by the Italian Ministry of University and Research (MIUR) within the Programma Operativo Nazionale 2000−2006 "Ricerca Scientifica, Sviluppo Tecnologico, Alta Formazione per le Regioni Italiane dell'Obiettivo 1 (Campania, Calabria, Puglia, Basilicata, Sicilia, Sardegna) Asse II, Misura II.2 Società dell'Informazione, Azione a Sistemi di calcolo e simulazione ad alte prestazioni".

Supporting Information Available: Simulated variations of the dipolar contribution to the observed ^{1}H chemical shift in WT horse cyano myoglobins. This material is available free of charge via the Internet at http://pubs.acs.org.

References and Notes

(1) Huang, Y. J.; Montelione, G. T. *Nature (London)* **2005**, *438*, 36–37.
(2) Tobi, D.; Bahar, I. *Proc. Natl. Acad. Sci. U.S.A.* **2005**, *102*, 18908–18913.
(3) Thornton, J. M.; Todd, A. E.; Milburn, D.; Borkakoti, N.; Orengo, C. A. *Nat. Struct. Biol.* **2000**, *7*, 991–994.
(4) Kendrew, J. C.; Parrish, R. G. *Proc. R. Soc. London A* **1956**, *238*, 305–324.
(5) Schoenborn, B. P.; Watson, H. C.; Kendrew, J. C. *Nature (London)* **1965**, *207*, 28–30.
(6) Tilton, R. F.; Kuntz, I. D.; Petsko, G. A. *Biochemistry* **1984**, *23*, 2849–2857.
(7) Tilton, R. F.; Singh, U. C.; Weiner, S. J.; Connolly, M. L.; Kuntz, I. D.; Kollman, P. A.; Max, N.; Case, D. A. *J. Mol. Biol.* **1986**, *192*, 443–456.
(8) Elber, R.; Karplus, M. *J. Am. Chem. Soc.* **1990**, *112*, 9161–9175.
(9) Scott, E. E.; Gibson, Q. H. *Biochemistry* **1997**, *36*, 11909–11917.
(10) Scott, E. E.; Gibson, Q. H.; Olson, J. S. *J. Biol. Chem.* **2001**, *276*, 5177–5188.
(11) Tetreau, C.; Di Primo, C.; Lange, R.; Tourbez, H.; Lavalette, D. *Biochemistry* **1997**, *36*, 10262–10275.
(12) Bertini, I.; Turano, P.; Vila, A. J. *Chem. Rev.* **1998**, *83*, 2833–2332.
(13) Bossa, C.; Anselmi, M.; Roccatano, D.; Amadei, A.; Vallone, B.; Brunori, M.; Di Nola, A. *Biophys. J.* **2004**, *86*, 3855–3862.
(14) Ceccarelli, M.; Ruggerone, P.; Anedda, R.; Casu, M.; Fais, A.; Era, B.; Sollaino, M. C.; Corda, M. *Biophys. J.* **2006**, *91*, 3529–3541.
(15) Emerson, S. D.; La Mar, G. N. *Biochemistry* **1990**, *29*, 1545–1556.
(16) Emerson, S. D.; La Mar, G. N. *Biochemistry* **1990**, *29*, 1556–1566.
(17) La Mar, G. N.; Cutnell, J. D.; Kong, S. B. *Biophys. J.* **1981**, *34*, 217–226.
(18) Yamamoto, Y.; Suzuki, T. *Biochim. Biophys. Acta* **1993**, *1163*, 287–296.
(19) Bondarenko, V.; Wang, J.; Kalish, H.; Balch, A. L.; La Mar, G. N. *J. Biol. Inorg. Chem.* **2005**, *10*, 283–293.
(20) Qin, J.; La Mar, G. N. *J. Biomol. NMR* **1992**, *2*, 597–618.
(21) Rajarathnam, K.; La Mar, G. N.; Chiu, M. L.; Sligar, S. G. *J. Am. Chem. Soc.* **1992**, *114*, 9048–9058.
(22) La Mar, G. N.; Walker, F. A. *J. Am. Chem. Soc.* **1973**, *95*, 1782–1790.
(23) Tetreau, C.; Blouquit, Y.; Novikov, E.; Quiniou, E.; Lavalette, D. *Biophys. J.* **2004**, *86*, 435–447.
(24) Tilton, R. F., Jr.; Kuntz, I. D., Jr. *Biochemistry* **1982**, *21*, 6850–6857.
(25) Bowers, C. R.; Storhaug, V.; Webster, C. E.; Bharatam, J.; Cottone, A., III; Gianna, R.; Betsey, K.; Gaffney, B. J. *J. Am. Chem. Soc.* **1999**, *121*, 9370–9377.
(26) Rubin, S. M.; Spence, M. M.; Goodson, B. M.; Wemmer, D. E.; Pines, A. *Proc. Natl. Acad. Sci. U.S.A.* **2000**, *97*, 3472–9475.
(27) Locci, E.; Dehouck, Y.; Casu, M.; Saba, G.; Lai, A.; Luhmer, M.; Reisse, J.; Bartik, K. *J. Magn. Reson.* **2001**, *150*, 167–174.
(28) Dubois, L.; Da Silva, P.; Landon, C.; Huber, J. G.; Ponchet, M.; Vovelle, F.; Berthault, P.; Desvaux, H. *J. Am. Chem. Soc.* **2004**, *126*, 15738–15746.
(29) Rubin, S. M.; Lee, S.-Y.; Ruiz, E. J.; Pines, A.; Wemmer, D. E. *J. Mol. Biol.* **2002**, *322*, 425–440.
(30) Gröger, C.; Möglich, A.; Pons, M.; Koch, B.; Hengstenberg, W.; Kalbitzer, H. R.; Brunner, E. *J. Am. Chem. Soc.* **2003**, *125*, 8726–8727.
(31) Mayer, A.; Ogawa, S.; Shulman, R. G.; Yamane, T.; Cavaleiro, J. A. S.; dA Rocha Gonsalves, A. M.; Kenner, G. W.; Smith, K. M. *J. Mol. Biol.* **1974**, *86*, 749–756.
(32) Shulman, R. G.; Peisach, J.; Wyluda, B. J. *J. Mol. Biol.* **1970**, *48*, 517–523.
(33) Medda, R.; Longu, S.; Anedda, R.; Padiglia, A.; Mura, A.; Casu, M.; Floris, G. *Biochimie* **2006**, *88*, 827–835.
(34) Mura, A.; Pintus, F.; Anedda, R.; Casu, M.; Padiglia, A.; Floris, G.; Medda, R. *FEBS J.* **2007**, *274*, 2585–2595.
(35) Anderson, M. A.; Xu, Y.; Grissom, C. B. *J. Am. Chem. Soc.* **2001**, *123*, 6720–6721.
(36) Anedda, R.; Soldatov, D. V.; Moudrakovski, I. L.; Casu, M.; Ripmeester, J. A. *Chem. Mater.* **2008**, *20*, 2908–2920.
(37) Preckel, A.; Weber, N. C.; Sanders, R. D.; Maze, M.; Schlack, W. *Anesthesiology* **2006**, *105*, 187–197.
(38) Preckel, B.; Schlack, W. *Best Pract. Res. Clin. Anaesthesiol.* **2005**, *19*, 365–379.
(39) Eckenhoff, R. G.; Johansson, J. S. *Pharm. Rev.* **1997**, *49*, 343–367.
(40) Nicholas Franks, P. *Nat. Rev. Neurosci.* **2008**, *9*, 370–386.
(41) Settle, W. Function of the myoglobin is influenced by anesthetic molecules. In *Guide to Molecular Pharmacology-Toxicology*; Featherstone, R. M., Ed.; Marcel Dekker: New York, 1973; Vol. 43.
(42) Nishihara, Y.; Sakakura, M.; Kimura, Y.; Terazima, M. *J. Am. Chem. Soc.* **2004**, *126*, 11877–11888.
(43) Corda, M.; Era, B.; Fais, A.; Casu, M. *Biochim. Biophys. Acta* **2004**, *1674*, 182–192.
(44) Rousseaux, J.; Dautrevaux, M.; Han, K. *Biochim. Biophys. Acta* **1976**, *439*, 55–62.
(45) Wittenberg, A.; Wittenberg, B. A. *Methods Enzymol.* **1981**, *76*, 29–33.
(46) Laemmli, U. K. *Nature (London)* **1970**, *227*, 680–685.
(47) Smith, D. W.; Williams, J. P. *Biochem. J.* **1968**, *110*, 297–301.
(48) Bax, A. *Two-Dimensional Nuclear Magnetic Resonance in Liquids*; Delft University Press: Delft, Holland, 1982.
(49) Jeener, J.; Meier, B. H.; Bachmann, P.; Ernst, R. R. *J. Chem. Phys.* **1979**, *71*, 4546–4553.
(50) Davis, D. G.; Bax, A. *J. Am. Chem. Soc.* **1985**, *107*, 2820–2821.
(51) Tilton, R. F., Jr.; Singh, U. C.; Weiner, S. J.; Connelly, M. L.; Kuntz, I. D., Jr.; Kollmann, P. A. *J. Mol. Biol.* **1986**, *192*, 443–456.
(52) Locci, E.; Casu, M.; Saba, G.; Lai, A.; Reisse, J.; Batik, K. *ChemPhysChem* **2002**, *3*, 812–814.
(53) Kurland, R. J.; McGarvey, B. R. *J. Magn. Reson.* **1970**, *2*, 286–301.
(54) Bertini, I.; Luchinat, C. *NMR of Paramagnetic Molecules in Biological Systems*; Benjamin Cummings Publishing Co.: Menlo Park, CA, 1986.
(55) Desvaux, H.; Dubois, L.; Huber, G.; Quillin, M. L.; Berthault, P.; Matthews, B. W. *J. Am. Chem. Soc.* **2005**, *127*, 11676–11683.
(56) Nisius, L.; Stadler, M.; Kalbitzer, H. R.; Brunner, E. *J. Phys. Chem. B* **2005**, *109*, 17795–17798.
(57) Mulder, F. A. A.; Hon, B.; Ranjith Muhandiram, D.; Dahlquist, F. W.; Kay, L. E. *Biochemistry* **2000**, *39*, 12614–12622.
(58) Kuriyan, J.; Wilz, S.; Karplus, M.; Petsko, G. A. *J. Mol. Biol.* **1986**, *192*, 133.
(59) Ringe, D.; Petsko, G. A.; Kerr, D. E.; Ortiz de Montellano, P. R. *Biochemistry* **1984**, *23*, 2–4.
(60) Mattevi, A.; Gatti, G.; Coda, A.; Rizzi, M.; Ascenzi, P.; Brunori, M.; Bolognesi, M. *J. Mol. Recognit.* **1991**, *4*, 1–6.
(61) Chacko, V. P.; La Mar, G. N. *J. Am. Chem. Soc.* **1982**, *104*, 7002–7007.
(62) Rajarathnam, K.; Qin, J.; La Mar, G. N.; Chiu, M. L.; Sligar, S. G. *Biochemistry* **1994**, *33*, 5493–5501.
(63) Wu, Y.; Chien, E. Y. T.; Sligar, S. G.; La Mar, G. N. *Biochemistry* **1998**, *37*, 6979–6990.
(64) Reisse, J. *New J. Chem.* **1986**, *10*, 665.
(65) Klug, D. D.; Zgierski, M. Z.; Tse, J. S.; Liu, Z.; Kincaid, J. R.; Czarnecki, K.; Hemley, R. J. *Proc. Natl. Acad. Sci. U.S.A.* **2002**, *99*, 12526–12530.
(66) Franzen, S.; Bohn, B.; Poyart, C.; DePillis, G.; Boxer, S. G.; Martin, J. L. *J. Biol. Chem.* **1995**, *270*, 1718–1720.

(67) Zhu, L.; Sage, J. T.; Champion, P. M. *Science* **1994**, *266*, 629–632.
(68) Schoenborn, B. P. *Mol. Pharmacol.* **1973**, *9*, 835–839.
(69) Cheng, X.; Schoenborn, B. P. *J. Mol. Biol.* **1991**, *220*, 381–399.
(70) Smerdon, S. J.; Krzywda, S.; Wilkinson, A. J.; Brantley, R. E., Jr.; Carver, T. E.; Hargrove, N. S.; Olson, J. S. *Biochemistry* **1993**, *32*, 5132–5138.
(71) Shiro, Y.; Iizuka, T.; Marubayashi, K.; Ogura, T.; Kitagawa, T.; Balasubramanian, S.; Boxer, S. G. *Biochemistry* **1994**, *33*, 14986–14992.
(72) Perutzand, M. F.; Matthews, F. S. *J. Mol. Biol.* **1966**, *21*, 199–202.
(73) Yang, F.; Philips, G. N., Jr. *J. Mol. Biol.* **1996**, *256*, 762–774.
(74) Lecomte, G. T. J.; La Mar, G. N. *J. Am. Chem. Soc.* **1987**, *109*, 7219–7220.
(75) Morishima, I.; Inubushi, T. *J. Am. Chem. Soc.* **1978**, *100*, 3568–3574.
(76) Cohen, J.; Arkhipov, A.; Braun, R.; Schulten, K. *Biophys. J.* **2006**, *91*, 1844–1857.
(77) Brunori, M.; Gibson, Q. H. *EMBO Rep.* **2001**, *2*, 674–679.
(78) Prangé, T.; Schiltz, M.; Pernot, L.; Colloc'h, N.; Longhi, S.; Bourguet, W.; Fourme, R. *Proteins: Struct. Funct. Bioinf.* **1998**, *30*, 61–73.

JP807959U